ROS

RESEARCH ARTICLES

Spontaneous Exit from Diplotene Arrest Associates with the Increase of Calcium and Reactive Oxygen Species in Rat Oocytes Cultured In Vitro

Meenakshi Tiwari and Shail K. Chaube

Cell Physiology Laboratory, Department of Zoology, Institute of Science, Banaras Hindu University, Varanasi-221005, U.P., India

Correspondence: shailchaubey@gmail.com (S.K.C.) or shailchaube@bhu.ac.in (S.K.C.)

Tiwari M and Chaube SK. Reactive Oxygen Species 4(12):418–433, 2017; ©2017 Cell Med Press
http://dx.doi.org/10.20455/ros.2017.865
(Received: August 5, 2017; Accepted: August 16, 2017)

ABSTRACT | Several signal molecules modulate the physiology of mammalian oocytes. Changes in the level of various signal molecules and their downstream impact on maturation promoting factor (MPF) during the achievement of meiotic competency remain ill understood. Therefore, the present study aimed to analyze levels of various signal molecules and MPF during the achievement of meiotic competency in rat oocytes. For this purpose, cumulus oocyte complexes (COCs) were collected from animals treated with 20 IU pregnant mare's serum gonadotropin (PMSG) for 48 h, followed by 20 IU human chorionic gonadotropin (hCG) for 14 h. The morphological changes, meiotic status and oocyte competency, cytosolic free calcium (Ca^{2+}), total reactive oxygen species (ROS), inducible nitric oxide synthase (iNOS), adenosine 3′,5′-cyclic monophosphate (cAMP), guanosine 3′,5′-cyclic monophosphate (cGMP), cell division cycle 25B (Cdc25B), calcium-calmodulin-dependent protein kinase II (CaMKII), Wee1, specific phosphorylation status of cyclin-dependent kinase 1 (Cdk1), and cyclin B1 expression levels were analyzed. Our data suggest that the culture of denuded diplotene-arrested oocytes resulted in spontaneous exit from diplotene arrest (EDA) in a time-dependent manner. The supplementation of hCG (2 IU) did not show any additive effect over spontaneous EDA in vitro. The hCG (20 IU) surge induced achievement of meiotic competency as most of the ovulated oocytes showed metaphase-II (M-II) arrest with extrusion of first polar body (PB-I). The spontaneous EDA was associated with a moderate increase of cytosolic free Ca^{2+} as well as total ROS levels. Furthermore, iNOS, cAMP, cGMP, Cdc25B, Thr161 phosphorylated Cdk1, as well as cyclin B1 levels were significantly decreased, while CaMKII, Wee1, and Thr14/Tyr15 phosphorylated Cdk1 levels were increased significantly during spontaneous EDA. These changes were reversed in ovulated oocytes that showed M-II arrest. The above results suggest that the oscillation of signal molecules modulates MPF destabilization during the achievement of meiotic competency in rat oocytes cultured in vitro.

KEYWORDS | Maturation promoting factor; Meiotic competency; Rat oocytes; Signal molecules

ABBREVIATIONS | ANOVA, analysis of variance; BCB, brilliant cresyl blue; CaMKII, calcium-calmodulin-dependent protein kinase II; cAMP, adenosine 3′,5′-cyclic monophosphate; CdK1, cyclin-dependent kinase 1; Cdc25B, cell division cycle 25B; cGMP, guanosine 3′,5′-cyclic monophosphate; COCs,

cumulus oocyte complexes; CTCF, corrected total cell fluorescence; EDA, exit from diplotene arrest; EDTA, ethylenediaminetetraacetic acid; FITC, fluorescein isothiocyanate; G6PDH, glucose-6-phosphate dehydrogenase; GV, germinal vesicle; GVBD, germinal vesicle breakdown; H_2DCFDA, 2′,7′-dichlorodihydrofluorescein diacetate; hCG, human chorionic gonadotropin; iNOS, inducible nitric oxide synthase; LH, luteinizing hormone; M-I, metaphase-I; M-II, metaphase-II; MPF, maturation promoting factor; PB-I, first polar body; PBS, phosphate-buffered saline; PI, propidium iodide; PMSG, pregnant mare's serum gonadotropin; ROS, reactive oxygen species; TRITC, tetramethylrhodamine isothiocyanate

CONTENTS

1. INTRODUCTION

Meiotic cell cycle in mammalian oocytes involves several stop/go channels [1–3]. Oocytes are physiologically arrested at diplotene stage within in the follicular microenvironment of mammalian ovary from birth to puberty [4–6]. These diplotene-arrested oocytes are morphologically identified by the presence of germinal vesicle (GV) and nucleolus [5, 7]. The diplotene arrest for such a long period is due to continuous transfer of several signal molecules and inhibitory factors via gap junctions from encircling granulosa cells to the oocyte [8, 9]. Pituitary gonadotropin surge disrupts gap junctions and cumulus-oocyte communications, which result interruption in the supply of several signal molecules and inhibitory factors to the oocyte resulting in meiotic exit from diplotene arrest (EDA) [10–12]. The physical removal of encircling granulosa cells also interrupts the supply of various signal molecules and inhibitory factors from granulosa cells to the oocyte and results in spontaneous EDA under in vitro culture conditions [13–18].

Achievement of meiotic competency starts with EDA and oocyte progresses into metaphase-I (M-I) stage [7, 12, 14, 17] and further gets physiologically arrested at metaphase-II (M-II) stage by extruding first polar body (PB-I) at the time of ovulation in most of the mammalian species [19–26]. These oocytes remain arrested at M-II stage even after ovulation until fertilization [2, 19, 22–26].

The meiotic competency of oocytes can be confirmed using brilliant cresyl blue (BCB) staining. Studies suggest that nicotinamide adenine dinucleo-

tide phosphate (NADPH) generated by glucose-6-phosphate dehydrogenase (G6PDH) in growing oocytes can reduce BCB stain, a phenoxazine compound and transform it to a colorless compound (leuco-phenoxazine) [27]. Thus, competent oocytes show decreased G6PDH and exhibit cytoplasm with blue coloration (BCB^+), whereas growing oocytes that are expected to have a high level of active G6PDH remain colorless (BCB^-) [28, 29]. Therefore, BCB staining has been used to classify competent oocytes in mice [30, 31], sheep [32], and cattle [33]. The human chorionic gonadotropin (hCG) surge triggers meiotic maturation in follicular oocytes and ovulation in various mammalian species during assisted reproductive technology (ART) programs [34]. The hCG mimics the action of luteinizing hormone (LH) and binds to LH receptors to trigger final maturation during last phases of folliculogenesis and thereby ovulation [34].

The meiotic maturation in follicular oocyte is modulated by several signal molecules [35]. These signal molecules are generated either by encircling granulosa cells or oocyte itself [8, 17, 36]. Different levels of these signal molecules probably decide whether the meiotic cell cycle has to be maintained at diplotene stage or progress inside the follicular microenvironment [6, 11, 22]. The calcium (Ca^{2+}), hydrogen peroxide (H_2O_2), inducible nitric oxide synthase (iNOS), adenosine 3′,5′-cyclic monophosphate (cAMP), and guanosine 3′,5′-cyclic monophosphate (cGMP) are major signal molecules that modulate meiotic cell cycle in mammalian oocytes [5, 6, 15–17]. These signal molecules could modulate cell division cycle 25B (Cdc25B), calcium-calmodulin-dependent protein kinase II (CaMKII), Wee1, maturation promoting factor (MPF) stabilization/destabilization, and/or cyclin-dependent kinase 1 (Cdk1) activity that may regulate meiotic cell cycle in oocytes [2, 15–17, 20–26, 35, 37]. However, the downstream impact of the signal molecules on MPF stabilization/destabilization during meiotic cell cycle progression from diplotene arrest to M-II arrest remains poorly understood. Therefore, the present study was aimed to analyze the changes and the potential impact of cytosolic free Ca^{2+}, total reactive oxygen species (ROS), iNOS, cAMP, cGMP, Cdc25B, CaMKII, Wee1, specific phosphorylation status of Cdk1, and cyclin B1 levels during achievement of meiotic competency in rat oocytes cultured in vitro.

2. MATERIAL AND METHODS

2.1. Chemicals and Preparation of Culture Medium

The culture medium (medium-199; AL094A, M-199) used in the present study was purchased from HiMedia Laboratories (Mumbai, India) and other chemicals were purchased from Sigma-Aldrich (St. Louis, MO, USA) unless otherwise stated. M-199 was prepared as per the company manual protocol. Sodium bicarbonate (0.035% w/v) was added, the pH was adjusted to 7.2 ± 0.05, and the osmolarity was checked (290 ± 5 m Osmol). The M-199 was then supplemented with glutamine, penicillin, and streptomycin (GPS; 1 µl/ml: Cat. No. A007, HiMedia) to prevent microbial growth and then stored at 4ºC until use (discarded if not used within 15 days). Plain M-199 was used for handling oocytes and washing purpose, while 5% fetal bovine serum (FBS) was added to M-199 and then used for in vitro studies.

2.2. Experimental Animal and Stimulation of Ovary

Immature female rats, *Rattus norvegicus*, of Charles-Foster strain (22–24 days old; 45 ± 5 g body weight) were housed in light-controlled room providing food and water ad libitum. Rats were subjected to a single subcutaneous injection of 20 IU pregnant mare's serum gonadotropin (PMSG) for 48 h or superovulation induction protocol (20 IU PMSG for 48 h followed by 20 IU hCG for 14 h). Thereafter, rats were euthanized and the ovary along with fallopian tube was collected in pre-warmed M-199. All procedures conformed in accordance with the institutional practice and within the framework of experimentation of animals (scientific procedure) Act of 2007, of the committee for the purpose of supervision and control on experiments on animals (CPSCEA), Government of India. The project was approved by Institutional Animal Ethical Committee of Institute of Science, Banaras Hindu University (wide letter no. F.Sc./IAEC/2014-15/0248).

2.3. Collection of Oocytes

In the first series of experiment, the ovary was punctured using a 26-gauge needle attached to a 1 ml of

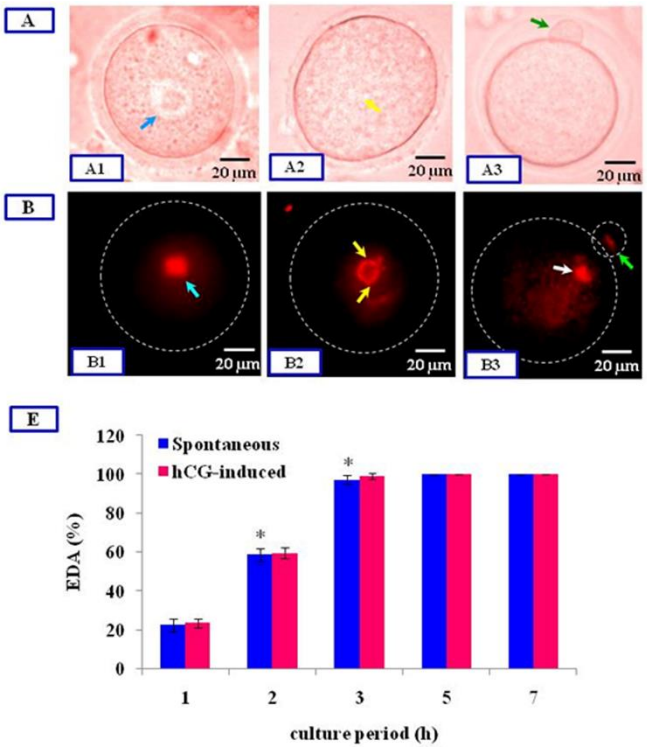

FIGURE 1. Representative photographs showing morphological changes in oocytes. Oocytes collected from PMSG-treated rats showed diplotene arrest as evidenced by the presence of GV and nucleolus (blue arrow, A1). Oocytes that underwent spontaneous EDA showed GVBD and absence of nucleolus (yellow arrow, A2) after 7 h of in vitro culture. Ovulated oocytes showed maintenance of M-II stage and PB-I extrusion (green arrow, A3) after 14 h of hCG surge. The diploid set of chromosomes confirmed the diplotene arrest (blue arrow, B1), while formation of metaphase plate (yellow arrows) specified spontaneous EDA (B2). M-II arrest was confirmed by one haploid set of chromosomes in oocyte cytoplasm (white arrow, B3) and another set of chromosomes in PB-I (green arrow, B3). Culture of diplotene-arrested oocytes with or without 2 IU hCG induced EDA in a time-dependent manner (C). Data are mean ± SEM of three independent experiments and analyzed by two-way ANOVA followed by Bonferroni post-hoc analysis. *, $P < 0.05$; bar = 20 µm.

tuberculin syringe under a microscope (Nikon type 104, Japan) in 35 mm Petri dish containing 2 ml of pre-warmed M-199. The diplotene-arrested COCs were collected after 48 h of PMSG (20 IU) surge using microtubing attached with a disposable glass micropipette (Clay Adams, NJ, USA). COCs were transferred to M-199 containing 0.01% hyaluronidase at 37ºC and denuded by repeated manual pipetting. The diplotene-arrested oocytes were identified morphologically by the presence of GV and nucleolus in oocyte cytoplasm.

To induce spontaneous EDA, diplotene-arrested oocytes were cultured for 7 h in vitro. The EDA was also induced by exposing diplotene-arrested oocytes to 2 IU hCG. The diplotene-arrested oocytes (18–20 oocytes in each group) were cultured with or without hCG for 1, 2, 3, 5, and 7 h in a CO_2 incubator (Galaxy 170R, New Brunswick, Eppendorf AG, Hamburg, Germany, UK; 37ºC temperature, 5% CO_2, and 100% humidity). Absence of GV was treated as EDA and used for further analysis in the present study.

For the collection of M-II arrested oocytes, rats were subjected to the superovulation induction protocol (20 IU PMSG for 48 h followed by 20 IU hCG for 14 h). The ovulated COCs were collected from ampulla of the fallopian tube and further cultured for

15 min in M-199 to induce the release of PB-I. COCs were denuded by repeated manual pipetting using 0.01% hyaluronidase. The presence of PB-I with normal morphology was treated as M-II arrested oocytes in the present study.

Approximately 12–14 oocytes from each group were washed three times with plain M-199 and then analyzed for morphological changes using a phase-contrast microscope (Nikon, Eclipse; E600, Tokyo, Japan) at 400× magnification. These oocytes were transferred on slide and fixed with 4% buffered formaldehyde for further analysis.

In the second series of experiments, in vitro studies were conducted as described for the first series and approximately 36–42 oocytes from each group were immediately used for the quantitative analysis of cAMP as well as cGMP levels. Three independent experiments were conducted using 76 experimental animals to get oocytes sufficient for morphological, biochemical, and immunofluorescence analysis in the present study.

2.4. Determination of Meiotic Status of Oocytes

The meiotic status of oocyte was confirmed using propidium iodide (PI) staining under a fluorescence microscope (Model, Ni-U, Nikon Eclipse Tokyo, Japan) as per previous published protocol [12]. For this purpose, approximately 12–14 oocytes collected from each group were washed 2 times with phosphate-buffered saline (PBS) and then incubated with PI (1 mg/ml) for 1 min in PBS. Thereafter, the oocytes were washed 5–6 times with PBS and then checked for their meiotic status under a fluorescence microscope at 540 nm (400× magnification). Three independent experiments were conducted to verify the meiotic stage and representative photographs are shown in the Results section.

2.5. Determination of Oocyte Meiotic Competency

The meiotic competency of oocytes was determined using BCB staining. For this purpose, a group of oocytes (12–14) were incubated with 26 µM of BCB diluted in M-199 for 30 min in a CO_2 incubator following previous published protocol with minor modifications [29]. At the end of the incubation period, oocytes were washed 3 times with PBS and then examined under a phase-contrast microscope for meiotic competency.

2.6. Analysis of Cytosolic Free Ca^{2+} and Total ROS Level

The cytosolic free Ca^{2+} and total ROS levels were analyzed using Fluo3/AM and 2′,7′-dichlorodihydrofluorescein diacetate (H_2DCFDA), respectively, following previous published protocol [22]. Briefly, 12-14 oocytes from each group were exposed to Fluo3/AM (50 µM) and H_2DCFDA (10 µM) for 30 min at 37ºC in a CO_2 incubator. Thereafter, oocytes were washed 3 times with pre-warmed PBS and then Fluo3 fluorescence was measured at 488 nm excitation/520 nm emission, and DCF fluorescence was measured at 485 nm excitation/520 nm emission using a fluorescence microscope (400× magnification). The corrected total cell fluorescence (CTCF) of 12-14 oocytes from three independent experiments was used for analysis using ImageJ software (version 1.44; the National Institutes of Health, Bethesda, USA).

2.7. Detection of iNOS, cAMP, Cdc25B, CaMKII, Wee1, Specific as well as Total Phosphorylation Status of Cdk1, and Cyclin B1 Expressions

Immunofluorescence of iNOS, cAMP, Cdc25B, CaMKII, Wee1, specific as well as total phosphorylation of Cdk1, and cyclin B1 expressions were analyzed in oocytes using their highly specific antibodies purchased from Santa Cruz Biotechnology (Dallas, TX, USA) as per our published protocol with some modifications [38]. In brief, 12–14 oocytes from each group were fixed with 4% buffered formaldehyde (10 min) at room temperature. Slides were washed 3 times with pre-warmed PBS and exposed to triton X-100 (0.01% in PBS) for 10 min at 37ºC. Slides were then treated with sodium citrate solution (0.01 M) at 37ºC (10 min). Slides were incubated with blocking buffer (2.5% PBS-BSA solution) at 37ºC (30 min). Thereafter, slides were exposed to 100 µl of their respective primary antibodies [NOS2 (N-20), rabbit polyclonal antibody (sc-651) raised against a peptide mapping near the N-terminus of NOS2; cAMP (AM01), mouse monoclonal antibody (sc-73761) raised against cAMP; Cdc25B (H- 85), rabbit polyclonal antibody (sc-5619) raised against amino acids 93-177 mapping near the N-terminus of Cdc25B; p-CaMKIIα (Thr286)-R, rabbit polyclonal antibody (sc-12886-R) raised against a short amino acid sequence contain

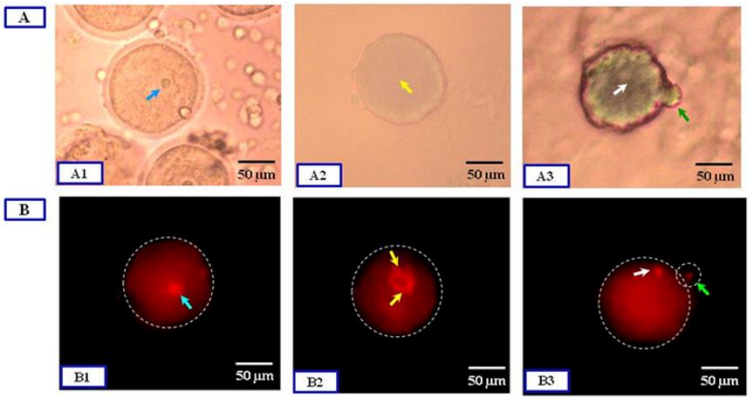

FIGURE 2. Representative photographs showing BCB staining in oocytes. The diplotene- arrested oocytes showing BCB- staining as the oocytes did not take any stain (blue arrow, A1). Oocytes that underwent spontaneous EDA showed BCB^+ stain as evidenced by faint blue colored cytoplasm (yellow arrow, A2). M-II arrested oocytes showed BCB^+ stain as evidenced by blue colored cytoplasm (white arrow, A3). The meiotic competency in oocytes was further confirmed by their meiotic status using PI staining (B1-3); bar = 50 µm.

ing phosphorylated Thr286 of CaMKIIα; Wee1 (H-300), rabbit polyclonal antibody (sc-9037) raised against amino acids 347-646 mapping at the C-terminus of Wee1; p-Cdc2 p34 (Thr14/Tyr15), rabbit polyclonal antibody (sc-12340) raised against a short amino acid sequence containing Thr14 and Tyr15 phosphorylated cdc2 p34; p-Cdc2 p34 (Thr161), rabbit polyclonal antibody (sc-12341) raised against a short amino acid sequence containing pThr161 of Cdc2 p-34; cdc2 p34 (PSTAIRE), rabbit polyclonal antibody (sc-53) raised against a peptide epitope mapping within the conserved PSTAIRE domain of cdc2 p34; cyclin B1 (H-433), rabbit polyclonal antibody (sc-752) raised against amino acids 1-433 representing full length of cyclin B1; Actin (C-2), mouse monoclonal antibody (sc-8432) specific for an epitope mapping between amino acids 350–375 at the C-terminous of actin; 1:500 dilutions in blocking buffer] at 37ºC for 1 h in a CO_2 incubator. After 6–8 washes with PBS, slides were exposed to 100 µl of specific anti-rabbit fluorescein isothiocyanate (FITC)-labeled (sc-3839) secondary antibody for detection of iNOS, Cdc25B, CaMKII, Wee1, Thr14/Tyr15, Thr161, as well as total phosphorylated Cdk1 and cyclin B1 levels, anti-mouse FITC-labeled (sc-2010) secondary antibody for detection of cAMP and anti-mouse tetramethylrhodamine isothiocyanate (TRITC)-labeled (sc-3796) secondary antibody for detection of β-actin at 37ºC a in humidified chamber (1:1000 dilutions in blocking buffer). After 1 h of incubation, slides were washed 6–8 times with pre-warmed PBS and then observed under a fluorescence microscope at 465 nm (FITC) and 540 nm (TRITC) at 400× magnification. Fluorescence intensity of β-actin was analyzed in parallel as a control to assure that all parameters were kept constant during immunofluorescence analysis. The experiment was repeated three times to confirm the results and the representative photographs are shown in the Result section.

2.8. Quantitative Estimation of cAMP and cGMP Concentrations

The cAMP as well as cGMP concentrations were analyzed using ELISA kits (cAMP: Cat. No. KGE002; cGMP: Cat. No. KGE003) purchased from R&D Systems (MN, USA) as per our previous published protocol [14]. In brief, approximately 36–42 oocytes collected from each group were lysed in hypotonic lysis buffer (5mM Tris, 20 mM ethylenediaminetetraacetic acid (EDTA), 0.5% TritonX-100, pH 8) and centrifuged at 10,000 × g at 4°C for 30 min. The supernatant was stored at –20°C until all samples were collected. Reagents, samples and standards were prepared as per the protocol provided by the company. The optical density (OD) was taken using a microplate reader (Model: Micro Scan MS5608A,

Electronics Corporation of India Limited, Hyderabad, India) set at 450 nm within 10 min. Samples from three independent experiments were run in one assay to avoid inter-assay variation and intra-assay variation was found to be 2.6 %. The cAMP as well as cGMP levels are represented as pmol/mg protein in the Results section.

2.9. Statistical Analyses

Data are expressed as mean ± standard error of mean (SEM) of three independent experiments. All percentage data were subjected to arcsine square-root transformation before statistical analysis and then analyzed either by Student's t-test or two-way analysis of variance (ANOVA) followed by Bonferroni post-hoc analysis using SPSS software, version 17.0 (SPSS, Inc., Chicago, IL, USA). A probability of $P < 0.05$ was considered statistically significant.

3. RESULTS

3.1. Morphological Changes in Oocytes During In Vitro Culture

As shown in **Figure 1**, oocytes collected from PMSG (20 IU for 48 h)-treated animals showed diplotene arrest as evidenced by the presence of GV and nucleolus (blue arrow; **Figure 1A1**). Oocytes showed germinal vesicle breakdown (GVBD, yellow arrow, **Figure 1A2**) during spontaneous as well as hCG (2 IU)-mediated EDA after 7 h of in vitro culture. The majority of oocytes were arrested at M-II stage and possess PB-I after 14 h of hCG surge (green arrow; **Figure 1A3**). The meiotic stages such as diplotene arrest (**Figure 1B1**), EDA (**Figure 1B2**), and M-II arrest (**Figure 1B3**) were further confirmed by their meiotic status using PI staining.

As shown in **Figure 1C**, culture of diplotene-arrested oocytes in medium supplemented with or without 2 IU hCG resulted in EDA in a time-dependent manner (two-way ANOVA, spontaneous EDA, $F = 380.51$; hCG-mediated EDA, $F = 382.34$, and interaction between these two factors, $F = 372.68$, $P < 0.001$, **Figure 1C**). hCG-induced EDA was similar to spontaneous EDA suggesting that 2 IU hCG neither had additive effect on EDA nor was sufficient to induce extrusion of PB-I under in vitro culture conditions. On the other hand, 20 IU hCG surge induced ovulation, extrusion of PB-I, and the majority of oocytes were arrested at M-II stage as evidenced by their chromosomal status (**Figure 1B3**).

3.2. Analysis of Meiotic Competency

The BCB test was conducted to determine whether oocytes were meiotically competent or not. Diplotene-arrested oocytes were BCB^- as the oocytes did not take any stain (**Figure 2A1**). Oocytes that showed EDA after 7 h of in vitro culture were meiotically competent as evidenced by BCB^+ faint blue staining (**Figure 2A2**). Furthermore, M-II arrested oocytes collected after 14 h hCG surge were also BCB^+ as the oocytes were stained blue (**Figure 2A3**). The meiotic competency in oocytes was further confirmed by their meiotic status using PI staining (**Figure 2B1-2B3**).

3.3. Changes in Ca^{2+} and ROS Levels

Figure 3 shows Fluo3 and DCF fluorescence intensity of Ca^{2+} and total ROS levels in oocytes. A moderate increase ($P < 0.001$) of Ca^{2+} and ROS levels was observed as evidenced by increase of fluorescence intensity in oocytes that underwent spontaneous EDA after 7 h of in vitro culture (**Figure 3A2** and **3C2**) as compared to diplotene-arrested oocytes (**Figure 3A1** and **3C1**). A significant decrease ($P < 0.01$) of Ca^{2+} as well as total ROS level was observed in M-II arrested oocytes collected after 14 h post-hCG surge (**Figure 3A3** and **3C3**) as compared to EDA oocytes (**Figure 3A2** and **3C2**). The CTCF analysis of oocytes using ImageJ software further confirmed our findings (**Figure 3B** and **3D**).

3.4. Changes in iNOS and Cyclic Nucleotides Expression Level

As shown in **Figure 4**, a significant decrease ($P < 0.001$) of iNOS (**Figure 4A2**), cAMP (**Figure 4C2** and **4E**) and cGMP (**Figure 4E**) levels were observed in oocytes that underwent spontaneous EDA as compared to their respective diplotene-arrested control oocytes (**Figure 4A1, 4C1,** and **4E**). Further, an increase ($P < 0.01$) of iNOS as well as cyclic nucleotides level were observed in M-II arrested oocytes collected after 14 h post-hCG surge (**Figure**

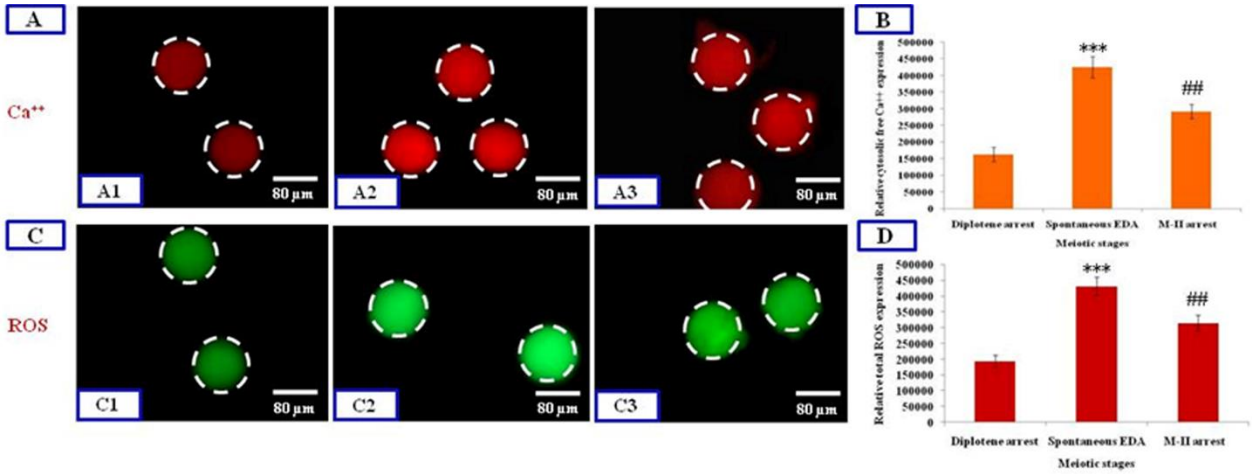

FIGURE 3. Representative photographs showing fluorescence intensity of cytosolic free Ca^{2+} as well as total ROS levels in oocytes. The Ca^{2+} and ROS levels were significantly increased in oocytes during spontaneous EDA (A2, C2) as compared to diplotene-arrested oocytes (A1, C1). The Ca^{2+} as well as total ROS level were significantly decreased in M-II arrested oocytes collected after 14 h post-hCG surge (A3, C3) as compared to EDA oocytes (A2, C2). The CTCF analysis of oocytes using ImageJ software further confirmed our results (B, D). Data are mean ± SEM of three independent experiments and analyzed by Student's t-test. *, $P < 0.001$, significantly increased (diplotene arrest versus spontaneous EDA); #, $p < 0.01$, significantly decreased (spontaneous EDA versus M-II arrest); bar = 80 µm.

4A3, 4C3, and **4E**) as compared to spontaneous EDA oocytes (**Figure 4A2, 4C2,** and **4E**). The CTCF analysis of iNOS and cAMP immunofluorescence further confirms our observations (**Figure 4B** and **4D**).

3.5. Changes in Cdc25B, CaMKII and Wee1 Expression Levels

As shown in **Figure 5**, a significant ($P < 0.001$) decrease of Cdc25B (**Figure 5A2**) and increase of CaMKII (**Figure 5C2**) and Wee1 (**Figure 5E2**) expression levels were observed in oocytes that underwent spontaneous EDA as compared to diplotene-arrested oocytes (**Figure 5A1, 5C1,** and **5E1**). The Cdc25B and Wee1 expression levels were increased significantly, while CaMKII expression level was decreased in M-II arrested oocytes collected after 14 h post-hCG surge (**Figure 5A3, 5C3,** and **5E3**) as compared to EDA oocytes (**Figure 5A2, 5C2,** and **5E2**). The CTCF analysis of their immunofluorescence intensity further confirmed our findings (**Figure 5B, 5D,** and **5F**).

3.6. Changes in Specific as well as Total Phosphorylation Status of Cdk1 and Cyclin B1 Levels

Figure 6 shows immunofluorescence intensity of total as well as specific phosphorylation status of Cdk1and cyclin B1 level in oocytes. A significant increase ($P < 0.001$) of immunofluorescence intensity of Thr14/Tyr15 phosphorylated Cdk1 level was observed in oocytes that underwent spontaneous EDA (**Figure 6A2**) as compared to diplotene-arrested oocytes (**Figure 6A1**). However, Thr14/Tyr15 specific immunofluorescence intensity was significantly increased ($P < 0.05$) in M-II arrested oocytes collected after 14 h post-hCG surge (**Figure 6A3**) as compared to EDA oocytes (**Figure 6A2**). Furthermore, a significant decrease ($P < 0.001$) of Thr161 phosphorylated Cdk1 level was observed in oocytes that underwent spontaneous EDA (**Figure 6C2**) as compared to diplotene-arrested oocytes (**Figure 6C1**). The Thr161 specific immunofluorescence intensity was increased significantly (P

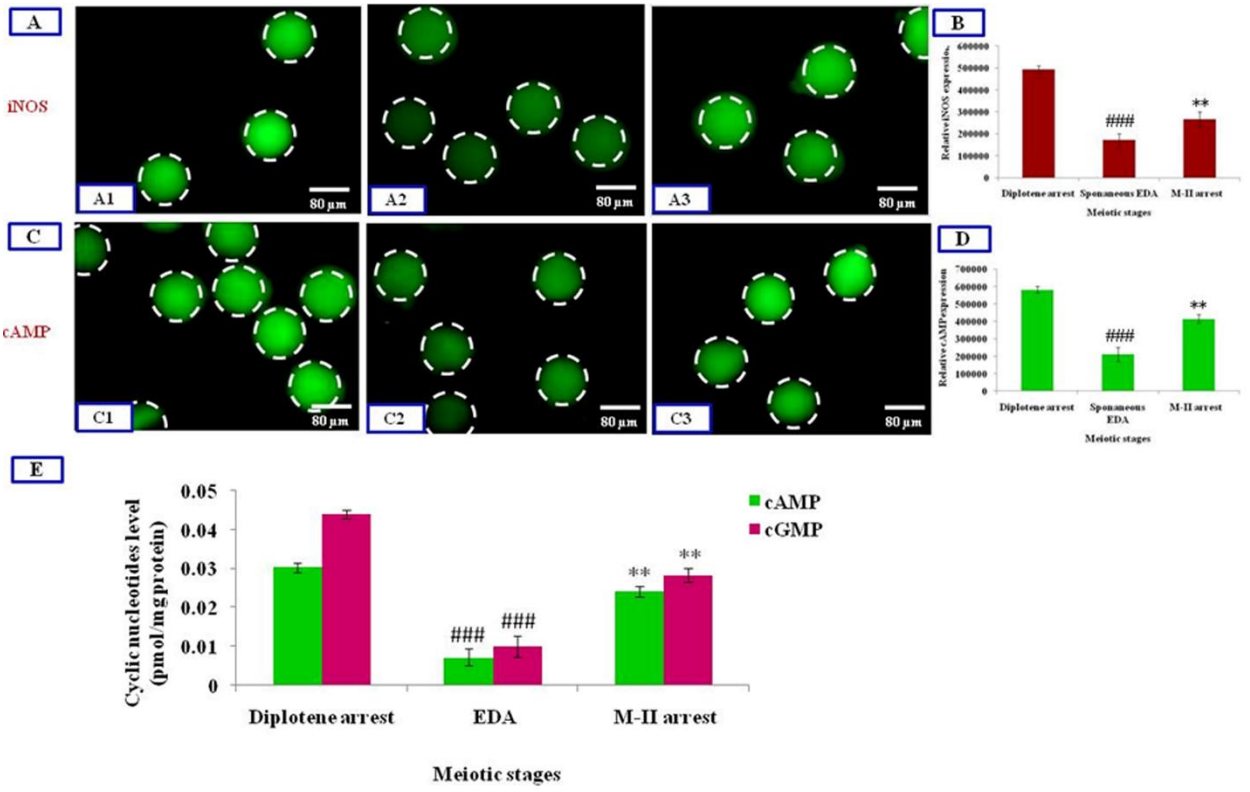

FIGURE 4. Representative photographs showing changes in iNOS and cyclic nucleotide level in oocytes. A significant decrease of iNOS (A2), cAMP (C2, E), and cGMP (E) levels was observed in oocytes during spontaneous EDA as compared to diplotene-arrested control oocytes (A1, C1, E). The iNOS as well as cyclic nucleotide level were significantly increased in M-II arrested oocytes (A3, C3, E) as compared to spontaneous EDA oocytes (A2, C2, E). The CTCF analysis of iNOS and cAMP immunofluorescence further confirmed our findings (B, D). Data are mean ± SEM of three independent experiments and analyzed by Student's t-test. #, $p < 0.001$, significantly decreased (diplotene arrest versus spontaneous EDA); *, $P < 0.01$, significantly increased (EDA versus M-II arrest); bar = 80 µm.

< 0.001) in M-II arrested oocytes (**Figure 6C3**). The total phosphorylated level (PSTAIRE) of Cdk1 did not alter during the achievement of meiotic competency (**Figure 6E1–6E3**). A significant reduction ($P < 0.001$) in cyclin B1 expression level was observed in oocytes that underwent spontaneous EDA (**Figure 6G2**) as compared to diplotene-arrested oocytes (**Figure 6G1**). However, cyclin B1 expression level was significantly increased ($P < 0.001$) in M-II arrested oocytes (**Figure 6G3**) as compared to EDA oocytes (**Figure 6G2**). The CTCF analysis further strengthened these observations (**Figure 6B, 6D, 6F,** and **6H**).

3.7. β-Actin Expression Remained Unchanged

The β-actin expression level was analyzed in parallel as a control for all the immunofluorescence studies. As shown in **Figure 7**, β-actin expression level did not change in oocytes of all groups (**Figure 7A1–7A3**). The CTCF analysis of further confirmed our observations (**Figure 7B**).

4. DISCUSSION

In mammals, oocyte quality is one of the most important factors that directly affects the outcome of

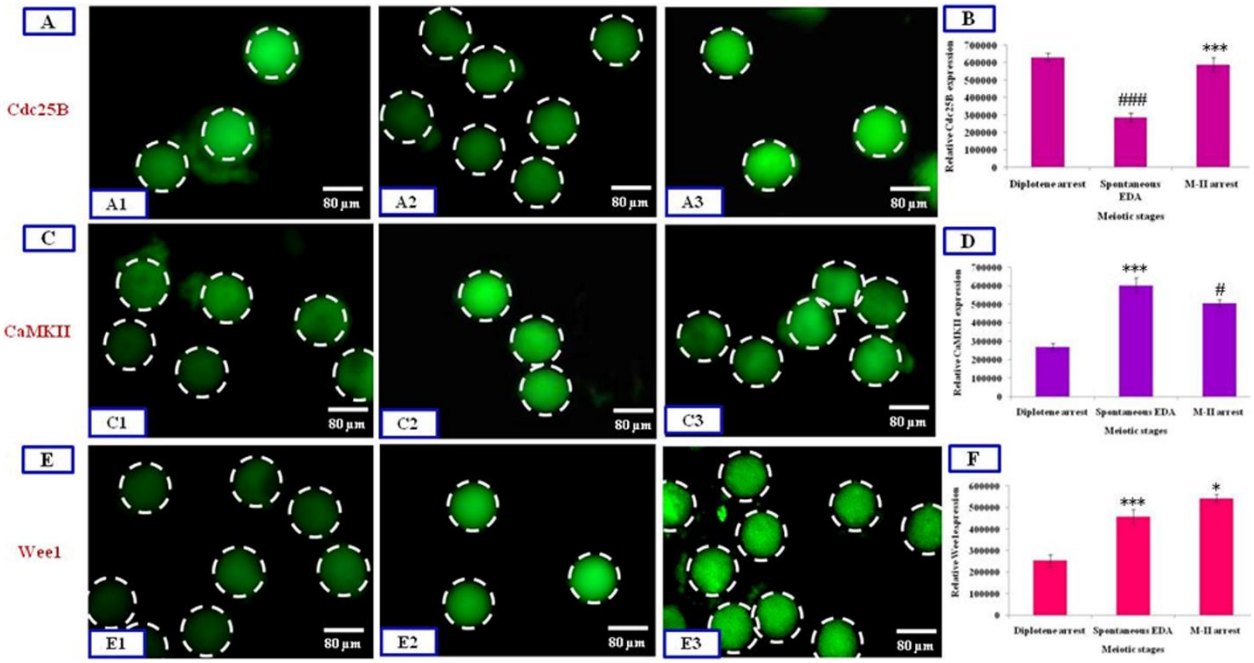

FIGURE 5. Representative photographs showing changes in Cdc25B, CaMKII, and Wee1 expression levels in oocytes. Spontaneous EDA in oocytes was associated with a decrease of Cdc25B (A2) and increase of CaMKII (C2) and Wee1 (E2) expression levels as compared to diplotene-arrested oocytes (A1, C1, E1). The Cdc25B and Wee1 expression levels were increased, while CaMKII expression level was decreased in M-II arrested oocytes collected after 14 h post-hCG surge (A3, C3, E3) as compared to EDA oocytes (A2, C2, E2). The CTCF analysis further strengthened our observations (B, D, F). Data are mean ± SEM of three independent experiments and analyzed by Student's t-test. Cdc25B, #, $p < 0.001$, significantly decreased; CaMKII and Wee1, *, $P < 0.001$, significantly increased (diplotene arrest versus spontaneous EDA); Cdc25B, *, $P < 0.001$, and Wee1, *, $P < 0.05$, significantly increased; CaMKII, #, $p < 0.05$, significantly decreased (spontaneous EDA versus M-II arrest); bar = 80 µm.

ARTs [3, 8, 39]. The oocyte quality is solely dependent upon the achievement of meiotic competency in oocyte, i.e., spontaneous EDA, progression via M-I to M-II stage, and release of PB-I that results in the production of haploid female gametes. The achievement of meiotic competency involves several biochemical and molecular changes [9, 39]. The successful completion of meiotic competency determines oocyte quality, which is a primary requirement for successful fertilization and early embryonic development [11–13, 39].

Pituitary gonadotropin surge is a prerequisite for the initiation of meiotic maturation in oocytes [1, 34]. Although hCG is frequently used as a surrogate for LH surge to induce ovulation in several mammalian species [34], its mechanism of action during achievement of meiotic competency remains ill understood. Our data suggested that almost 95% oocytes collected after 48 h PMSG surge were arrested at diplotene stage. Culture of these oocytes in vitro resulted in spontaneous EDA in a time-dependent manner. hCG-induced EDA was similar to spontaneous EDA suggesting that 2 IU hCG neither had additive effect on EDA nor was sufficient to induce extrusion of PB-I under in vitro culture conditions. On the other hand, the superovulation induction protocol induced achievement of meiotic competency as evidenced by the extrusion of PB-I in more than 95% of oocytes collected from ampulla of fallopian tube and further cultured for 10–15 min in M-199 under in

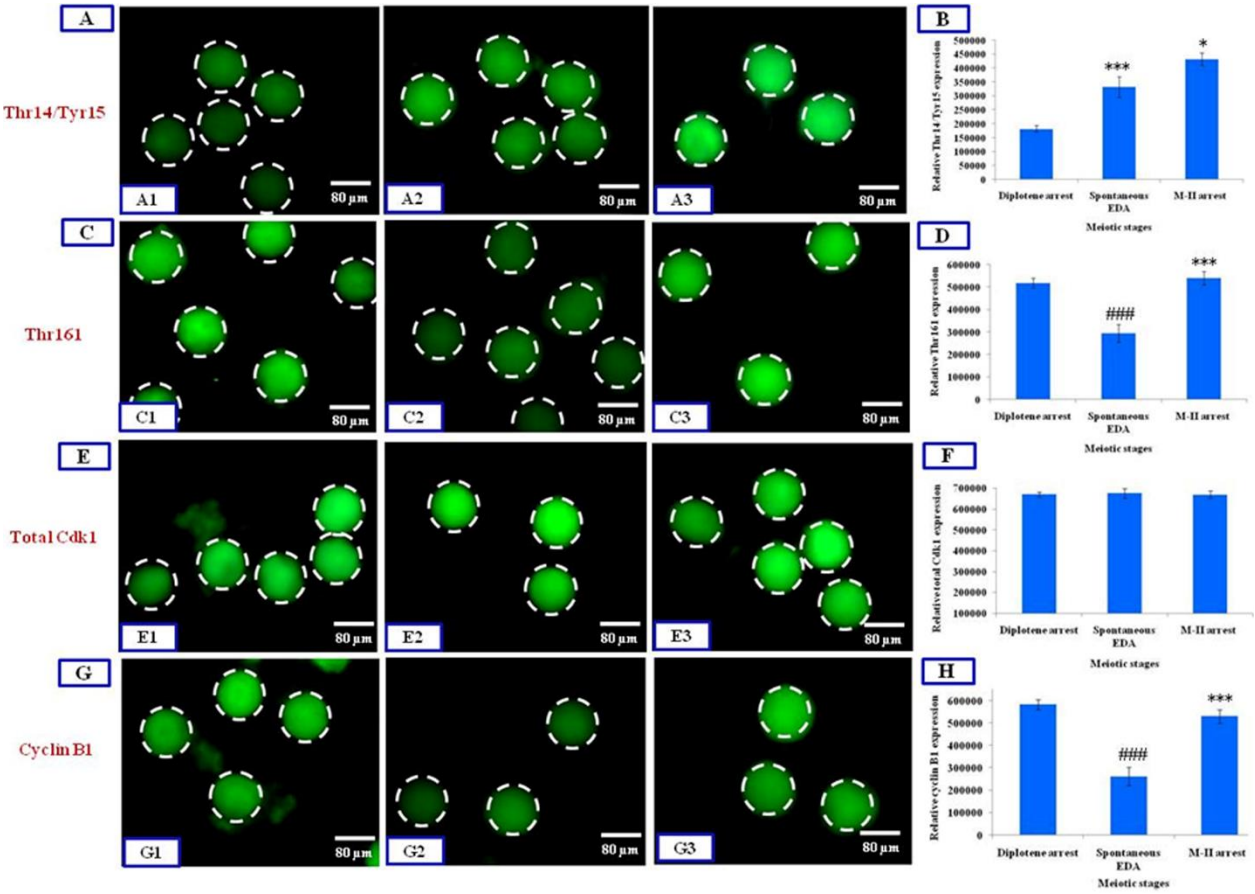

FIGURE 6. Representative photographs showing changes in specific as well as total phosphorylation status of Cdk1 and cyclin B1 expression levels in oocytes. An increase of Thr14/Tyr15 phosphorylated Cdk1 level was observed during spontaneous EDA (A2) and then it was further increased in M-II arrested oocytes collected after 14 h post-hCG surge (A3) as compared to EDA oocytes (A2). The Thr161 phosphorylated Cdk1 level was decreased during spontaneous EDA (C2) and then further increased in M-II arrested oocytes (C3). The total phosphorylated level (PSTAIRE) remained unchanged during the achievement of meiotic competency (E1-3). The cyclin B1 expression level was reduced during spontaneous EDA (G2) as compared to diplotene-arrested oocytes (G1), but increased in M-II arrested oocytes (G3). The CTCF analysis further strengthened our findings (B, D, F, H). Data are mean ± SEM of three independent experiments and analyzed by Student's t-test. Thr14/Tyr15, *, $P < 0.001$, significantly increased; Thr161 and cyclin B1, #, $p < 0.001$, significantly decreased (diplotene arrest versus EDA); Thr14/Tyr15, *, $P < 0.05$, and Thr161 and cyclin B1, *, $P < 0.001$, significantly increased (spontaneous EDA versus M-II arrest); bar = 80 µm.

vitro culture conditions. These results suggest that hCG is not effective in inducing EDA under in vitro culture conditions as compared to in vivo surge. The hCG was not effective under in vitro culture conditions possibly due to the removal of mural granulosa cell encircling oocyte at the time of oocyte collection in the present study. The encircling mural granulosa cells provide the site of hCG action as they have specific receptors on the cell membrane [1, 4, 9, 10].

The meiotic competency of oocytes was confirmed using BCB staining in the present study. BCB test is an indirect measure of oocyte growth that allows the

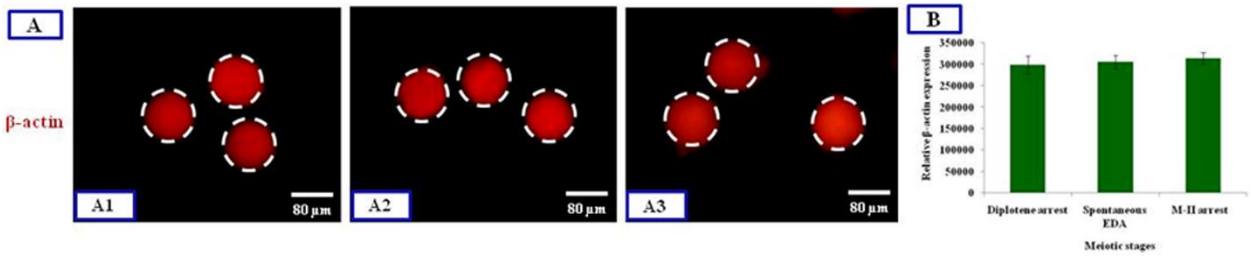

FIGURE 7. Representative photographs showing β-actin expression in oocytes. The β-actin expression level did not change in oocytes during the entire course of study (A1-A3). The CTCF analysis of further confirmed our observations (B); bar = 80 µm.

selection of competent oocytes during in vitro maturation [30]. Data of the present study suggested that diplotene-arrested oocytes had a high G6PDH activity as these oocytes did not take any stain (BCB^-). Oocytes that showed EDA after 7 h of in vitro culture had little amount of active G6PDH as evidenced by faint blue BCB stain (BCB^+). However, M-II arrested oocytes collected after 14 h hCG surge showed decreased G6PDH and exhibited cytoplasm with blue BCB^+ stain, suggesting that these oocytes have achieved meiotic competency. Similarly, BCB staining has been used to select competent oocytes in mice, sheep, and cattle [31–33].

The increased Ca^{2+} oscillations trigger EDA in mouse and pig oocytes [40–42]. Our data show a moderate increase of cytosolic free Ca^{2+} level in oocytes that underwent spontaneous EDA after 7 h of in vitro culture. However, Ca^{2+} level was decreased in M-II arrested oocytes collected after 14 h post-hCG surge. These results are further supported by the observations that increased cytosolic free Ca^{2+} level participates in meiotic cell cycle progression from diplotene arrest in rat [22], mouse [43], caprine [44], and bovine oocytes cultured in vitro [45].

A moderate increase of intracellular Ca^{2+} ($[Ca^{2+}]_i$) level under the physiological range triggers generation of ROS and decreases iNOS expression during spontaneous EDA in rat oocytes cultured in vitro [14, 22, 46–48]. Our results suggested that increase of ROS level and decrease of iNOS expression induced EDA after 7 h of in vitro culture. An increase of ROS and decrease of iNOS expression level were associated with the decrease of cyclic nucleotide level during spontaneous EDA [9, 12, 14, 49]. Our results suggested that the increased cytosolic free Ca^{2+} as well as ROS levels were associated with decreased cAMP as well as cGMP levels during spontaneous EDA. However, the level of both cyclic nucleotides was increased in M-II arrested oocytes collected after 14 h post-hCG surge. Based on these results, we propose that a moderate increase of Ca^{2+} as well as ROS and decrease of iNOS, cAMP, as well as cGMP levels mediate spontaneous EDA, while the reverse changes were associated with the maintenance of M-II arrest. Similarly, the increased level of ROS and decreased level of cyclic nucleotides have been reported during spontaneous EDA in rat and human oocytes [9, 12, 14, 22, 49].

Reduction of the level of both cyclic nucleotides could modulate the downstream pathway(s) to destabilize MPF by altering Cdc25B and Wee1 activities in oocytes. A reduction of cGMP level activates cAMP-phosphodiesterase 3A (PDE 3A) and reduces intraoocyte cAMP level [50, 51]. The reduced intraoocyte cAMP level may result in inactivation of Cdc25B and activation of Wee1 kinase that destabilize MPF leading to EDA in several mammalian species [4, 52]. This possibility is further supported by the observations that the increased intraoocyte cAMP level activates protein kinase A (PKA), which phosphorylates Cdc25B phosphatase [51, 52]. Data of our present study suggested that the Cdc25B expression level was reduced in oocytes that underwent spontaneous EDA in vitro. On the other hand, Wee1 kinase expression level was increased during 7 h of in vitro culture. These data suggest that the inactivation of Cdc25B and activation of Wee1 kinase associate with spontaneous EDA in rat oocytes in vitro.

A moderate increase of Ca^{2+} as well as ROS level destabilizes MPF [46, 49]. Increase of Ca^{2+} and ROS level triggers activation of CaMKII [48]. The CaMKII activates Wee1 that destabilizes MPF by inducing phosphorylation of Thr14/Tyr15 of Cdk1 and triggers degradation of cyclin B1 [40]. The destabilized MPF and/or Cdk1 activity triggers EDA in rat and sheep oocytes [12, 14, 22, 32, 38]. Data of the present study suggested that the increase of cytosolic free Ca^{2+} and total ROS levels increased CaMKII expression, which thereby increased Wee1 and Thr14/Tyr15 phosphorylated Cdk1 expression level. On the other hand, Thr161 phosphorylated Cdk1 and cyclin B1 levels decreased significantly during EDA. However, the total Cdk1 level did not change. These results suggested a moderate increase of Ca^{2+} and ROS levels modulated specific phosphorylation status of Cdk1 and triggered EDA. Similarly, changes in specific phosphorylation status of Cdk1 have been reported during EDA in rat [14, 22] and mouse oocytes cultured in vitro [52, 53].

In conclusion, our results suggested that a moderate increase of Ca^{2+} as well as ROS levels and decrease of cyclic nucleotide level mediated spontaneous EDA during the achievement of meiotic competency in rat oocytes. The reduced cyclic nucleotide level decreased Cdc25B expression level, which resulted in the increase of CaMKII, Wee1, as well as Thr14/Tyr15 phosphorylated Cdk1 level. However, Thr161 phosphorylated Cdk1 as well as cyclin B1 levels were reduced significantly leading to MPF destabilization. The destabilized MPF finally resulted in spontaneous EDA in rat oocytes cultured in vitro. Thus, a moderate increase of Ca^{2+} as well as ROS levels under the physiological range and transient decrease of cyclic nucleotide level destabilize MPF that finally leads to the achievement of meiotic competency in mammalian oocytes.

ACKNOWLEDGMENTS

M.T. conducted experiments under the guidance of S.K.C. Both of the authors read and finalized the manuscript. This study was financially supported by Department of Science and Technology, Ministry of Science and Technology of India (Grant No. EMR/2014/000702). The authors declare no potential conflicts of interest with respect to the research, authorship, and/or publication of this article.

REFERENCES

1. Zhang M, Ouyang H, Xia G. The signal pathway of gonadotrophins-induced mammalian oocyte meiotic resumption. *Mol Hum Reprod* 2009; 15(7):399–409. doi: 10.1093/molehr/gap031.
2. Tripathi A, Kumar KV, Chaube SK. Meiotic cell cycle arrest in mammalian oocytes. *J Cell Physiol* 2010; 223(3):592–600. doi: 10.1002/jcp.22108.
3. Chaube SK, Prasad S, Tiwari M, Gupta A. Rat: an interesting model to study oocyte meiosis in mammals. *RRJZS* 2016; 4(3):25–7.
4. Chen ZQ, Ming TX, Nielsen HI. Maturation arrest of human oocytes at germinal vesicle stage. *J Hum Reprod Sci* 2010; 3(3):153–7. doi: 10.4103/0974-1208.74161.
5. Pandey AN, Tripathi A, Premkumar KV, Shrivastav TG, Chaube SK. Reactive oxygen and nitrogen species during meiotic resumption from diplotene arrest in mammalian oocytes. *J Cell Biochem* 2010; 111(3):521–8. doi: 10.1002/jcb.22736.
6. Tiwari M, Prasad S, Tripathi A, Pandey AN, Singh AK, Shrivastav TG, et al. Involvement of reactive oxygen species in meiotic cell cycle regulation and apoptosis in mammalian oocytes. *Reactive Oxygen Species* 2016; 1(2):110–6. doi: 10.20455/ros.2016.817
7. Mrazek M, Fulka Jr J, Jr. Failure of oocyte maturation: possible mechanisms for oocyte maturation arrest. *Hum Reprod* 2003; 18(11):2249–52.
8. Wigglesworth K, Lee KB, O'Brien MJ, Peng J, Matzuk MM, Eppig JJ. Bidirectional communication between oocytes and ovarian follicular somatic cells is required for meiotic arrest of mammalian oocytes. *Proc Natl Acad Sci USA* 2013; 110(39):E3723–9. doi: 10.1073/pnas.1314829110.
9. Nunes C, Silva JV, Silva V, Torgal I, Fardilha M. Signalling pathways involved in oocyte growth, acquisition of competence and activation. *Hum Fertil (Camb)* 2015; 18(2):149–55. doi: 10.3109/14647273.2015.1006692.
10. Huang Z, Wells D. The human oocyte and cumulus cells relationship: new insights from the cumulus cell transcriptome. *Mol Hum Reprod* 2010; 16(10):715–25. doi: 10.1093/molehr/gaq031.

11. Li R, Albertini DF. The road to maturation: somatic cell interaction and self-organization of the mammalian oocyte. *Nat Rev Mol Cell Biol* 2013; 14(3):141–52. doi: 10.1038/nrm3531.
12. Tiwari M, Chaube SK. Moderate increase of reactive oxygen species triggers meiotic resumption in rat follicular oocytes. *J Obstet Gynaecol Res* 2016; 42(5):536–46. doi: 10.1111/jog.12938.
13. Uyar A, Torrealday S, Seli E. Cumulus and granulosa cell markers of oocyte and embryo quality. *Fertil Steril* 2013; 99(4):979–97. doi: 10.1016/j.fertnstert.2013.01.129.
14. Pandey AN, Chaube SK. Reduction of nitric oxide level leads to spontaneous resumption of meiosis in diplotene-arrested rat oocytes cultured in vitro. *Exp Biol Med (Maywood)* 2015; 240(1):15–25. doi: 10.1177/1535370214545024.
15. Tiwari M, Prasad S, Pandey AN, Premkumar KV, Tripathi A, Gupta A, et al. Nitric oxide signaling during meiotic cell cycle regulation in mammalian oocytes. *Front Biosci (Schol Ed)* 2017; 9:307–18.
16. Tiwari M, Prasad S, Shrivastav TG, Chaube SK. Calcium signaling during meiotic cell cycle regulation and apoptosis in mammalian oocytes. *J Cell Physiol* 2017; 232(5):976–81. doi: 10.1002/jcp.25670.
17. Gupta A, Tiwari M, Prasad S, Chaube SK. Role of cyclic nucleotide phosphodiesterases during meiotic resumption from diplotene arrest in mammalian oocytes. *J Cell Biochem* 2017; 118(3):446–52. doi: 10.1002/jcb.25748.
18. Tiwari M, Chaube SK. Carbenoxolone reduces cyclic nucleotides level, destabilizes maturation promoting factor and induces meiotic exit from diplotene arrest in rat cumulus oocytes complexes cultured in vitro. *Biomed Pharmacother* 2017; 94:219–30. doi: 10.1016/j.biopha.2017.07.097.
19. Kubiak JZ, Ciemerych MA, Hupalowska A, Sikora-Polaczek M, Polanski Z. On the transition from the meiotic to mitotic cell cycle during early mouse development. *Int J Dev Biol* 2008; 52(2–3):201–17. doi: 10.1387/ijdb.072337jk.
20. Premkumar KV, Chaube SK. Nitric oxide signals postovulatory aging-induced abortive spontaneous egg activation in rats. *Redox Rep* 2015; 20(4):184–92. doi: 10.1179/1351000215Y.0000000003.
21. Premkumar KV, Chaube SK. Increased level of reactive oxygen species persuades postovulatory aging-mediated spontaneous egg activation in rat eggs cultured in vitro. *In Vitro Cell Dev Biol Anim* 2016; 52(5):576–88. doi: 10.1007/s11626-016-0007-3.
22. Prasad S, Tiwari M, Tripathi A, Pandey AN, Chaube SK. Changes in signal molecules and maturation promoting factor levels associate with spontaneous resumption of meiosis in rat oocytes. *Cell Biol Int* 2015; 39(6):759–69. doi: 10.1002/cbin.10444.
23. Prasad S, Tiwari M, Koch B, Chaube SK. Morphological, cellular and molecular changes during postovulatory egg aging in mammals. *J Biomed Sci* 2015; 22:36. doi: 10.1186/s12929-015-0143-1.
24. Prasad S, Tiwari M, Pandey AN, Shrivastav TG, Chaube SK. Impact of stress on oocyte quality and reproductive outcome. *J Biomed Sci* 2016; 23:36. doi: 10.1186/s12929-016-0253-4.
25. Prasad S, Tiwari M, Chaube SK. Abortive spontaneous egg activation: an emerging biological threat for the existence of mammals. *Cell Reprogram* 2017; 19(3):145–9. doi: 10.1089/cell.2016.0052.
26. Tiwari M, Tripathi A, Chaube SK. Presence of encircling granulosa cells protects against oxidative stress-induced apoptosis in rat eggs cultured in vitro. *Apoptosis* 2017; 22(1):98–107. doi: 10.1007/s10495-016-1324-4.
27. Palmer T, Jackson JB. A rapid burst preceding the steady-state rate of H^+-transhydrogenase during illumination of chromatophores of *Rhodobacter capsulatus*: implications for the mechanism of interaction between protonmotive force and enzyme. *FEBS Lett* 1990; 277(1–2):45–8.
28. Tiwari M, Chaube SK. Increase of reactive oxygen species associates with the achievement of meiotic competency in rat oocytes cultured in vitro. *Reactive Oxygen Species* 2017; 4(11) (in press). doi: 10.20455/ros.2017.853.
29. Azari-Dolatabad N, Rahmani HR, Hajian M, Ostadhosseini S, Hosseini SM, Nasr-Esfahani MH. Effects of cilostamide and/or forskolin on the meiotic resumption and development competence of growing ovine oocytes selected by brilliant cresyl blue staining. *Theriogenology*

2016; 85(8):1483–90. doi: 10.1016/j.theriogenology.2016.01.008.
30. Mangia F, Epstein CJ. Biochemical studies of growing mouse oocytes: preparation of oocytes and analysis of glucose-6-phosphate dehydrogenase and lactate dehydrogenase activities. *Dev Biol* 1975; 45(2):211–20.
31. Salimi M, Salehi M, Masteri Farahani R, Dehghani M, Abadi M, Novin MG, et al. The effect of melatonin on maturation, glutathione level and expression of H MGB1 gene in brilliant cresyl blue (BCB) stained immature oocyte. *Cell J* 2014; 15(4):294–301.
32. Catala MG, Izquierdo D, Uzbekova S, Morato R, Roura M, Romaguera R, et al. Brilliant cresyl blue stain selects largest oocytes with highest mitochondrial activity, maturation-promoting factor activity and embryo developmental competence in prepubertal sheep. *Reproduction* 2011; 142(4):517–27. doi: 10.1530/REP-10-0528.
33. Opiela J, Katska-Ksiazkiewicz L, Lipinski D, Slomski R, Bzowska M, Rynska B. Interactions among activity of glucose-6-phosphate dehydrogenase in immature oocytes, expression of apoptosis-related genes Bcl-2 and Bax, and developmental competence following IVP in cattle. *Theriogenology* 2008; 69(5):546–55. doi: 10.1016/j.theriogenology.2007.11.001.
34. Theofanakis C, Drakakis P, Besharat A, Loutradis D. Human Chorionic Gonadotropin: The pregnancy hormone and more. *Int J Mol Sci* 2017; 18(5). doi: 10.3390/ijms18051059.
35. Adhikari D, Liu K. The regulation of maturation promoting factor during prophase I arrest and meiotic entry in mammalian oocytes. *Mol Cell Endocrinol* 2014; 382(1):480–7. doi: 10.1016/j.mce.2013.07.027.
36. Tiwari M, Prasad S, Tripathi A, Pandey AN, Ali I, Singh AK, et al. Apoptosis in mammalian oocytes: a review. *Apoptosis* 2015; 20(8):1019–25. doi: 10.1007/s10495-015-1136-y.
37. Madgwick S, Jones KT. How eggs arrest at metaphase II: MPF stabilisation plus APC/C inhibition equals Cytostatic Factor. *Cell Div* 2007; 2:4. doi: 10.1186/1747-1028-2-4.
38. Tiwari M, Chaube SK. Maturation promoting factor destabilization mediates human chorionic gonadotropin induced meiotic resumption in rat oocytes. *Develop Growth Differ* 2017.
39. Liu W, Xin Q, Wang X, Wang S, Wang H, Zhang W, et al. Estrogen receptors in granulosa cells govern meiotic resumption of pre-ovulatory oocytes in mammals. *Cell Death Dis* 2017; 8(3):e2662. doi: 10.1038/cddis.2017.82.
40. Fan HY, Huo LJ, Meng XQ, Zhong ZS, Hou Y, Chen DY, et al. Involvement of calcium/calmodulin-dependent protein kinase II (CaMKII) in meiotic maturation and activation of pig oocytes. *Biol Reprod* 2003; 69(5):1552–64. doi: 10.1095/biolreprod.103.015685.
41. Silvestre F, Boni R, Fissore RA, Tosti E. Ca^{2+} signaling during maturation of cumulus-oocyte complex in mammals. *Mol Reprod Dev* 2011; 78(10–11):744–56. doi: 10.1002/mrd.21332.
42. Yoon J, Juhn KM, Yoon SH, Ko Y, Lim JH. Effects of sperm insemination on the final meiotic maturation of mouse oocytes arrested at metaphase I after in vitro maturation. *Clin Exp Reprod Med* 2017; 44(1):15–21. doi: 10.5653/cerm.2017.44.1.15.
43. Hwang H, Cheon YP. Adenosine receptors mediated intracellular calcium in cumulus cells involved in the maintenance of first meiotic arrest. *Dev Reprod* 2013; 17(2):141–7. doi: 10.12717/DR.2013.17.2.141.
44. Zhou HM, Jin SY. Ca^{2+} cascade and meiotic resumption of the caprine primary oocyte. *Reprod Domest Anim* 2007; 42(5):555–9. doi: 10.1111/j.1439-0531.2006.00824.x.
45. Boni R, Cuomo A, Tosti E. Developmental potential in bovine oocytes is related to cumulus-oocyte complex grade, calcium current activity, and calcium stores. *Biol Reprod* 2002; 66(3):836–42.
46. Tosti E. Calcium ion currents mediating oocyte maturation events. *Reprod Biol Endocrinol* 2006; 4:26. doi: 10.1186/1477-7827-4-26.
47. Basini G, Grasselli F. Nitric oxide in follicle development and oocyte competence. *Reproduction* 2015; 150(1):R1–9. doi: 10.1530/REP-14-0524.
48. Gorlach A, Bertram K, Hudecova S, Krizanova O. Calcium and ROS: a mutual interplay. *Redox Biol* 2015; 6:260–71. doi: 10.1016/j.redox.2015.08.010.
49. Cheon YP, Kim SW, Kim SJ, Yeom YI, Cheong C, Ha KS. The role of RhoA in the germinal vesicle breakdown of mouse oocytes. *Biochem*

Biophys Res Commun 2000; 273(3):997–1002. doi: 10.1006/bbrc.2000.3052.

50. Wang Y, Teng Z, Li G, Mu X, Wang Z, Feng L, et al. Cyclic AMP in oocytes controls meiotic prophase I and primordial folliculogenesis in the perinatal mouse ovary. *Development* 2015; 142(2):343–51. doi: 10.1242/dev.112755.
51. Egbert JR, Uliasz TF, Shuhaibar LC, Geerts A, Wunder F, Kleiman RJ, et al. Luteinizing hormone causes phosphorylation and activation of the cGMP phosphodiesterase PDE5 in rat ovarian follicles, contributing, together with PDE1 activity, to the resumption of meiosis. *Biol Reprod* 2016; 94(5):110. doi: 10.1095/biolreprod.115.135897.
52. Solc P, Schultz RM, Motlik J. Prophase I arrest and progression to metaphase I in mouse oocytes: comparison of resumption of meiosis and recovery from G2-arrest in somatic cells. *Mol Hum Reprod* 2010; 16(9):654–64. doi: 10.1093/molehr/gaq034.
53. Adhikari D, Busayavalasa K, Zhang J, Hu M, Risal S, Bayazit MB, et al. Inhibitory phosphorylation of Cdk1 mediates prolonged prophase I arrest in female germ cells and is essential for female reproductive lifespan. *Cell Res* 2016; 26(11):1212–25. doi: 10.1038/cr.2016.119.